



**HAL**  
open science

# Assessment of Diffusion Parameters of New Passive Samplers Using Optical Chemical Sensor for On-Site Measuring Formaldehyde in Indoor Air: Experimental and Numerical Studies

J. Vignau-Laulhere, Pierre Mocho, H. Plaisance, K. Raulin, V. Desauziers

## ► To cite this version:

J. Vignau-Laulhere, Pierre Mocho, H. Plaisance, K. Raulin, V. Desauziers. Assessment of Diffusion Parameters of New Passive Samplers Using Optical Chemical Sensor for On-Site Measuring Formaldehyde in Indoor Air: Experimental and Numerical Studies. *Analytical and Bioanalytical Chemistry*, 2016, 408 (8), pp.2147-2157. <10.1007/s00216-016-9317-2>. <hal-02129512>

**HAL Id: hal-02129512**

**<https://hal.science/hal-02129512v1>**

Submitted on 2 Nov 2023

HAL is a multi-disciplinary open access archive for the deposit and dissemination of scientific research documents, whether they are published or not. The documents may come from teaching and research institutions in France or abroad, or from public or private research centers.

L'archive ouverte pluridisciplinaire HAL, est destinée au dépôt et à la diffusion de documents scientifiques de niveau recherche, publiés ou non, émanant des établissements d'enseignement et de recherche français ou étrangers, des laboratoires publics ou privés.



HAL Authorization

# Assessment of diffusion parameters of new passive samplers using optical chemical sensor for on-site measuring formaldehyde in indoor air: experimental and numerical studies

Jane Vignau-Laulhere<sup>1,2</sup> · Pierre Mocho<sup>3</sup> · Hervé Plaisance<sup>2</sup> · Katarzyna Raulin<sup>1</sup> · Valérie Desauziers<sup>2</sup>

**Abstract** New passive samplers using a sensor consisting of a sol-gel matrix entrapping Fluoral-P as sampling media were developed for the determination of formaldehyde in indoor air. The reaction between Fluoral-P and formaldehyde produces a colored compound which is quantified on-site by means of a simple optical reading module. The advantages of this sensor are selectivity, low cost, ppb level limit of detection, and on-site direct measurement. In the development process, it is necessary to determine the sampling rate, a key parameter that cannot be directly assessed in the case of diffusive samplers using optical chemical sensor. In this study, a methodology combining experimental tests and numerical modeling is proposed and applied at five different radial diffusive samplers equipped with the same optical chemical sensor to assess the sampled material flows and sampling rates. These radial diffusive samplers differ in the internal volume of the sampler (18.97 and 6.14 cm<sup>3</sup>), the position of sensor inside the sampler (in front and offset of 1.2 cm above the membrane) and the width of the diffusion slot (1.4 and 5.9 mm). The influences of these three parameters (internal volume, position of sensor inside the sampler, and width of the diffusion slot) were assessed and discussed with regard to the formaldehyde sampling rate and water uptake by sensor (potential interference of measure). Numerical simulations based on Fick's laws are in agreement with the experimental results and provide to

estimate the effective diffusion coefficient of formaldehyde through the membrane ( $3.50 \times 10^{-6} \text{ m}^2 \text{ s}^{-1}$ ). Conversion factors between the sensor response, sampled formaldehyde mass and sampling rate were also assessed.

**Keywords** Radial diffusive samplers · Gas sensor · Fluoral-P · Sampling rate · Mass transfer modeling

## Introduction

Among indoor air pollutants, formaldehyde is of particular interest due to its abundance in indoor air and to its adverse effects on health [1]. Formaldehyde was classified as a human carcinogen by the International Agency for Research on Cancer (IARC, 2006) and plays a role in the triggering of some respiratory diseases like asthma [2] and lower respiratory infections and nocturnal dry cough in infancy [3, 4]. Formaldehyde is emitted by various off-gassing sources such as building materials and furniture, especially those containing urea, phenolic and melamine resins [5–7]. In France, two national measurement campaigns conducted from 2003 to 2005 in 567 dwellings and from 2009 to 2011 in 316 day-care centers and primary schools showed that formaldehyde was the most abundant detected VOCs with mean concentrations of 19.6 and 15.7  $\mu\text{g m}^{-3}$ , respectively [8]; 22 % of dwellings exceeded the upcoming French regulation threshold of 30  $\mu\text{g m}^{-3}$  for long-term exposure.

Today, standard methods to measure formaldehyde concentrations are based on the collection by active or passive sampling using cartridges impregnated with 2,4-dinitrophenylhydrazine followed by HPLC analysis of the formed hydrazones (NF ISO 16000-3, 2002). Other techniques exist like chemical sensors [9, 10], gas sensors based on metal oxides [11, 12] piezoelectric sensors [13, 14]

---

✉ Valérie Desauziers  
valerie.desauziers@mines-ales.fr

<sup>1</sup> Ethera, 7 Parvis Louis Néel, 38040 Grenoble, Cedex 9, France

<sup>2</sup> Pôle RIME-C2MA, Ecole des Mines d'Alès, Hélioparc, 2 Avenue Pierre Angot, 64053 Pau, Cedex 9, France

<sup>3</sup> Laboratoire Thermique Énergétique et Procédés, Université de Pau et des Pays de l'Adour, BP Pau 7511-64053, France

enzyme-based biosensors [7, 15], SPME on-fiber derivatization with O-(2,3,4,5,6-pentafluorobenzyl) hydroxylamine [16, 17], and reaction with dansylhydrazine [18].

With the aim to extend the monitoring of formaldehyde indoors, there is a need for a simple method which supplies on-site measurements without analysis in laboratory with a selectivity and sensibility adequate for indoor air. Few methods among those above mentioned are able to meet these technical requirements. Colorimetric sensors based on the Hantzsch reaction between 4-amino-3-penten-2-one (Fluoral-P) and formaldehyde appears as the most promising technical path. This reaction leads to the formation of 3,5-diacetyl-1,4-dihydrolutidine (DDL) which is a fluorescent compound. The rate of DDL formation can be measured by fluorescence or absorption [19]. Although the fluorescence technique has a higher sensibility, absorption is preferred for on-site measurements because it is less expensive than fluorescence. Two sensors based on Fluoral-P and formaldehyde reaction exist: for one, the reagent is adsorbed into the porous glass [20] and for the other one, Fluoral-P is entrapped in a nanoporous monolith [21]. The sensor response is an absorbance change converted in formaldehyde concentration from empirical relationship set up in calibration enclosure or by field comparison with another method (like DNPH-derivatization method) [22]. When these sensors are used as trapping media into passive samplers, the absorbance change cannot be easily translated into collected mass of formaldehyde and the sampling rate of diffusive sampler remains mostly unknown. However, the sampling rate and the correspondence between the absorbance change and collected mass are useful particularly to assist in understanding the causes of certain sensor response deviations. The sensor response includes the contributions of various processes (diffusions, sorption, reaction, and measurement by spectrophotometry) with no possibility to distinguish them.

The present study proposes an original approach based on experimental tests supplemented by a numerical modeling for assessing sampled material flow and sampling rate of diffusive samplers with optical chemical sensor. The methodology can be generalized to all types of passive samplers with optical chemical sensor. It is here applied to five radial diffusive samplers of different geometrical characteristics using the same chemical sensor doped with Fluoral-P. The sampling rates of five diffusive samplers and the correspondence absorbance change/collected mass were experimentally assessed. These sampling rates were modeled with numerical simulations based on Fick's laws and compared to the experimental results and discussed. The sensor is a nanoporous silica gel monolith which is a hydrophilic absorbent so water can potentially be an interfering of measure. In consequence, water flows transferred to the sensor were also experimentally assessed and modeled.

## Materials and methods

### ETHERA® passive samplers


Five prototypes of diffusive sampler having different geometric characteristics (internal volume, diffusion slot, and position of trapping media in the passive sampler) were designed and evaluated (Fig. 1).

All diffusive samplers have a diffusion membrane which is a micro porous polyethylene cylinder of 27.6 mm in diameter, 10 mm long, 3.2 mm wall thickness, and a mean radius of 5  $\mu\text{m}$  pore size. Two diffusion slots are symmetrically arranged on the outer surface of the membrane. Two widths of diffusion slot were tested, 1.4 and 5.9 mm corresponding to a membrane exposed external surface of 96 and 404  $\text{mm}^2$ . Two plastic components hold the membrane and ensure the airtightness.

The tested diffusive samplers have two different internal volumes: QAI samplers (QAI 1.4, QAI 5.9, and QAI 1.4dep) have an internal volume of 18.97  $\text{cm}^3$  and LDE samplers of 6.14  $\text{cm}^3$ . A nanoporous sensor is placed inside a plastic rod, itself inserted into the sampler body for sampling. The radius of monolith is 2.2 mm, internal and external radius of the membrane 10.5 mm and 13.7 mm, respectively. So the radial distance between the external surfaces of monolith and membrane is equal to 11.5 mm, according to Fig. 6. For the two samplers QAI 1.4 and QAI 5.9, the sensor is placed at the same level as the membrane whereas for the three samplers LDE 1.4, LDE 5.9 and QAI 1.4dep, the sensor is shifted by 1.2 cm upwards relative to the membrane. This sensor is a parallelepipedal monolith with a surface available for sampling of 125.4  $\text{mm}^2$ . The chemical sensor is a nanoporous monolithic matrix which is prepared from the Sol-Gel process [23], using tetramethyl orthosilicate (TMOS) and (3-aminopropyl)triethoxysilane (APTES) as precursors and Fluoral-P (98 % pure) as active molecule [24]. Formaldehyde in presence of water vapor reacts with the Fluoral-P to produce a colored compound, 3,5-diacetyl-1,4-dihydrolutidine (DDL) [25]. This method allows the detection

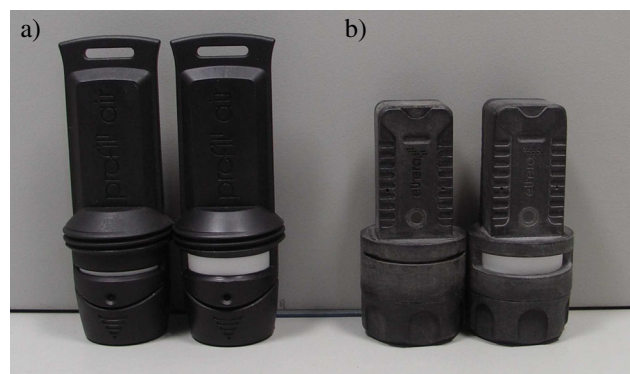
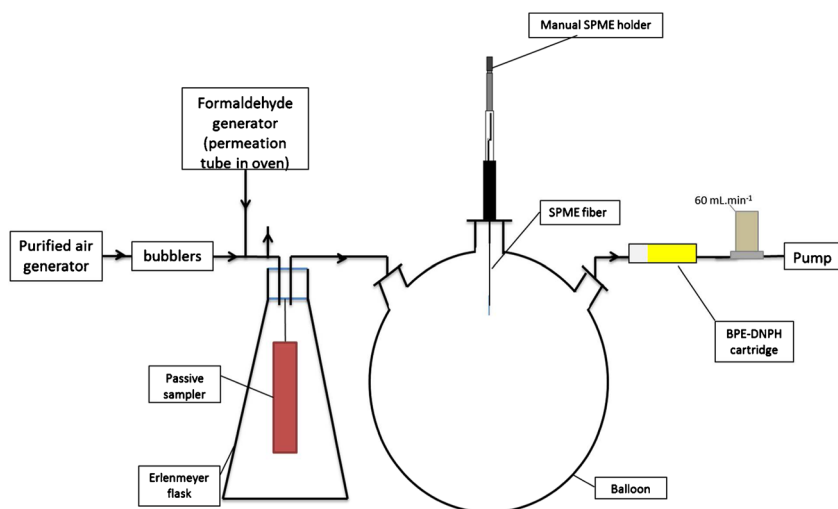


**Fig. 1** a) QAI samplers with slot of 1.4 and 5.9 mm and (b) LDE samplers with slot of 1.4 and 5.9 mm

**Fig. 2** Layout of the experimental setup:  = mass flow controller



of formaldehyde at ppb level in indoor air [9]. DDL formed is quantified by an absorbance measure of monolith at 420 nm by means of an optical reading module. The absorbance is proportional to the DDL amount formed. The chemical reaction kinetics is known to be fast so its formation can be correlated to the sampled formaldehyde mass.

For all devices, the mass transfer of formaldehyde is controlled by two main steps: an effective diffusion of compound through the porous membrane, defined by an effective diffusion coefficient ( $D_M$ ) and the diffusion of formaldehyde in gaseous phase ( $D_G$ ). It also depends on the concentration gradient that takes place between the air outside the sampler and the sensor. The mass transfer of water vapor is mainly influenced by the adsorption capacity of the monolith, due to high level of this compound in air (some  $\text{g m}^{-3}$ ) and the limited monolith surface. To take this state into account, a monolith/gas adsorption equilibrium is considered at the monolith surface.

### Determination of the formaldehyde sampling rate and formaldehyde diffusion coefficient through the membrane

In the case of diffusive samplers using optical chemical sensor, the sampling rate cannot be assessed by the classical tests in exposure chamber because the optical response does not inform on the sampled material flow and sampling rate. Therefore, an experimental device was set up to deduce sampled material flow from the difference between inlet and outlet concentrations of a dynamic system in which the sampler is placed.

For that, each ETHERA passive sampler is placed in a closed 2-L Erlenmeyer flask for 1 day in which the formaldehyde concentration [HCHO] in inlet air is controlled as shown in Fig. 2.

The material flow sampled by each passive sampler ( $F_{\text{HCHO}}$ ,  $\mu\text{g min}^{-1}$ ) was calculated according to the following equation available in steady state:

$$F_{\text{HCHO}} = F_{\text{air}}(C_0 - C_S) \quad (12)$$

Where  $F_{\text{air}}$  is the air flow ( $\text{m}^3 \text{min}^{-1}$ ),  $C_0$  the formaldehyde concentration ( $\mu\text{g m}^{-3}$ ) in inlet air, and  $C_S$  formaldehyde concentration ( $\mu\text{g m}^{-3}$ ) in outlet air. The air flow stream inside the Erlenmeyer flask is assumed to be turbulent and consequently the formaldehyde concentration ( $C_S$ ) is considered as homogeneous in this area.

The experimental sampling rate of formaldehyde ( $\text{SR}_{\text{exp}}$ ,  $\text{mL min}^{-1}$ ) was calculated according to the following equation:

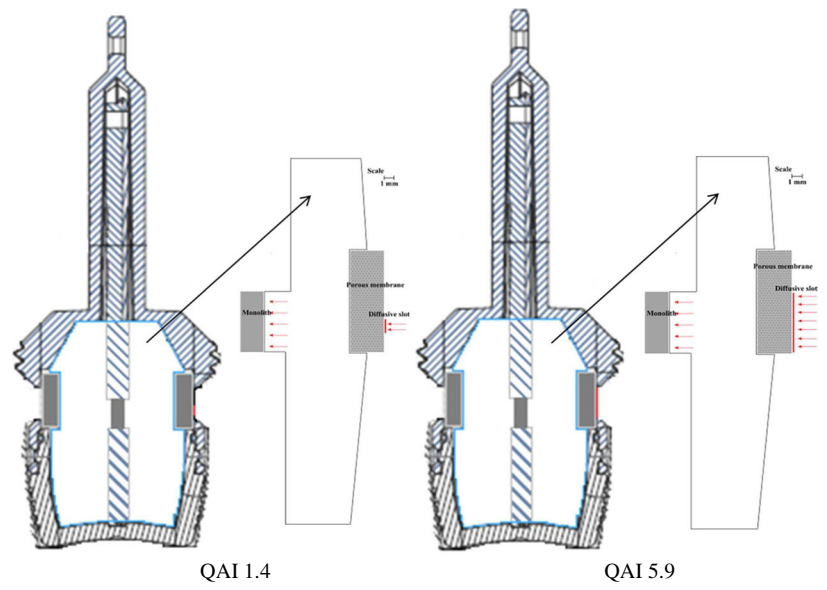
$$\text{SR}_{\text{exp}} = \frac{F_{\text{HCHO}}}{C_S} \times 10^6 \quad (13)$$

The effective diffusion coefficient ( $D_M$ ) used in the model is deduced by fitting to the experimental sampling rates ( $\text{SR}_{\text{exp}}$ ).

The experiment was repeated three times for each passive sampler (twice for the passive sampler QAI 1.4dep).

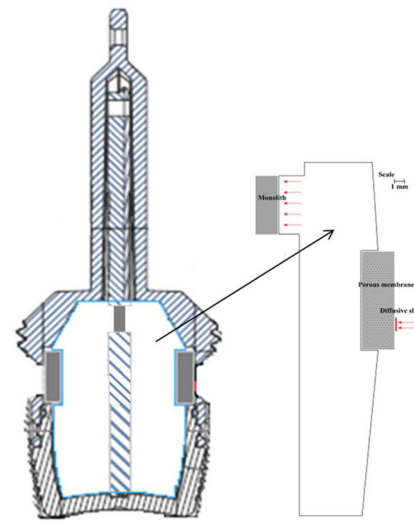
Air flushing the Erlenmeyer is produced by an experimental setup comprising a compressor, an air purifier (Claind, Lenno, Italy) and a permeameter manufactured by Calibrage (Saint Chamas, France). A first air flow consisted of dry air with a stable formaldehyde concentration is produced by a permeameter equipped by a paraformaldehyde permeation tube Dynacal® (VICI Metronics, Washington, USA). A second air flow comes from a humidifier system consisting in bubblers filled up with water and flushed with purified air. A third air flow supplies dry air for dilution and humidity setting. These three airflows are regulated by mass flow controllers. They are mixed at the Erlenmeyer inlet, generating controlled

**Fig. 3** Plans and half cross section of passive samplers used for modeling

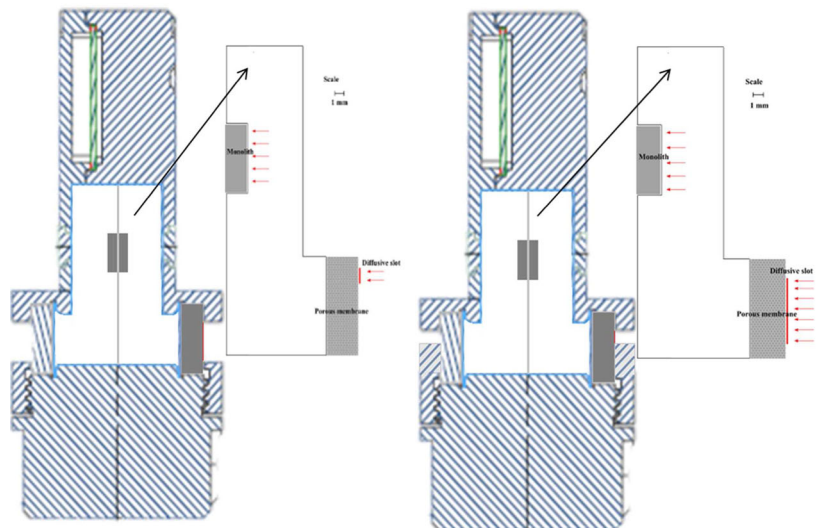


QAI 1.4

QAI 5.9



QAI 1.4 dep



LDE 1.4

LDE 5.9

atmospheres with a formaldehyde concentration of about  $30 \mu\text{g m}^{-3}$  and relative humidity of  $50.0 \pm 3.2 \%$ . The inlet airflow is regulated to  $60 \text{ mL min}^{-1}$ . The experimental setup is placed in air-conditioned room at regulated temperature ( $20 \pm 1 \text{ }^\circ\text{C}$ ). The inlet and outlet formaldehyde concentrations in the experimental setup are monitored by two different techniques, both the SPME method and active sampling method in order to ensure the measurement.

The formaldehyde concentrations are determined by SPME on-fiber derivatization followed by GC/FID analysis. A polydimethylsiloxane-divinylbenzene (PDMS-DVB) ( $65 \mu\text{m}$ ) (Supelco, Bellefonte, PA, USA) SPME fiber impregnated with *o*-(2,3,4,5,6-pentafluorobenzyl)hydroxylamine (PFBHA) (Fluka, Brucks, Switzerland) is used. The development and the performance of this method are described in previous articles [17, 26]. The impregnated fiber is exposed to the air in the balloon for 10 min. The amount of formaldehyde is determined by GC/FID according to the method described in the paragraph “GC/FID analysis”.

The formaldehyde concentrations are also monitored by a 24-h sample pumped on dual-bed 1,2-bis(2-pyridyl)ethylene/DNPH (BPE/DNPH) cartridges (Sigma-Aldrich, Saint Louis, MO, USA) developed by Uchiyama [27]. The active sampling covers full sampling duration. Air sample is first drawn through the BPE bed and then through the DNPH one. This cartridge allows simultaneous quantification of ozone which reacts with BPE (no use for our tests) and carbonyls which reacts with DNPH. The sampling flow rate was regulated to  $60 \text{ mL min}^{-1}$  with a mass flow meter and checked before and after each pumped sample with a gas flow meter (DryCal DC-Lite, Butler, NJ, USA). Preliminary tests showed that in this configuration, no breakthrough occurs. The cartridges are extracted in the reverse direction to air sampling with 3 mL of a mixture composed of 30 % of dimethyl sulfoxide (DMSO) and 70 % of acetonitrile with an added aliquot of phosphoric acid (0.085 % (v/v)). Acetonitrile (>99.9 %) and DMSO (>99.7 %) were supplied by Sigma-Aldrich (Saint Louis, MO, USA), phosphoric acid was provided by Carlo Erba Reagents (Val de Reuil, France). The amount of formaldehyde is determined by HPLC from the analysis of its formed hydrazone according to the method described in the next paragraph, “HPLC analysis”.

### HPLC analysis

The extracts of active cartridges were analyzed with a common protocol by HPLC on a Thermo Fisher Scientific

**Table 2** Adsorption isotherm of water vapor onto modified silica gel monolith—parameters of the Peleg model

Parameter	Value
A	$3.912 \times 10^{-8}$
B	$7.548 \times 10^{-2}$
C	5.1
D	$7.0 \times 10^{-3}$

Ultimate 3000 with a UV/Vis detector (Thermo Fisher Scientific, MA, USA) at 349 nm. Analyses of formaldehyde are carried out using Ascentis RP-Amide,  $5 \mu\text{m}$  particle size,  $250 \text{ mm} \times 4.6 \text{ mm}$  i.d. column (Supelco, Bellefonte, PA, USA). The mobile phase was composed of acetonitrile/MilliQ water (34/66 (v/v)) at a flow rate of  $2 \text{ mL min}^{-1}$  and the injection volume was  $20 \mu\text{L}$ . More details on the analysis method are given by Uchiyama et al. [28].

### GC/FID analysis

A CP-3800 GC gas chromatograph (Varian, Les Ulis, France) equipped with a split/splitless injection port and a flame ionization detector (FID) was used. The split/splitless injection port was equipped with  $0.75 \text{ mm}$  i.d. liner. The injector operated in splitless mode and the temperature was  $250 \text{ }^\circ\text{C}$ . A  $60 \text{ m} \times 0.25 \text{ mm}$  i.d. Optima-5 Accent fused silica column with a  $1 \mu\text{m}$  film thickness was used (Macherey-Nagel, Düren, Germany) was used. The GC temperature was  $40 \text{ }^\circ\text{C}$  (4 min hold) to  $90 \text{ }^\circ\text{C}$  at  $15 \text{ }^\circ\text{C min}^{-1}$  (4 min hold), then to  $250 \text{ }^\circ\text{C}$  at  $10 \text{ }^\circ\text{C min}^{-1}$  (5 min hold). Helium was used as carrier gas and the flow rate was  $2 \text{ mL min}^{-1}$ . More details on the preparation of the impregnated fiber and the analysis method are given by Bourdin et al. [17].

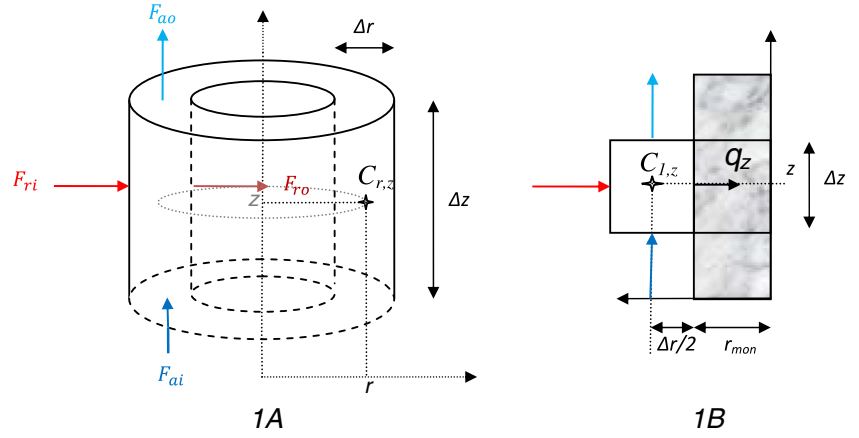
### Experimental setup (follow-up water uptake trapped by the sensor)

To determine the water flows trapped by sensor, each sampler is put on a microbalance itself placed in a closed enclosure in which relative humidity (RH) is controlled. This enclosure of 57 L is flushed with humidified purified air at a flow rate of  $4 \text{ L min}^{-1}$  allowing to rapidly reach 80 % ( $13.82 \text{ g m}^{-3}$ ,  $20 \text{ }^\circ\text{C}$ , and 1 atm) and to maintain it. The experimental setup is also placed in air-conditioned room at regulated temperature ( $20 \pm 1 \text{ }^\circ\text{C}$ ). The follow up the sampler weight is carried out for 24 h.

**Table 1** Main inlet parameters of the computer program

Discretization parameters			$D_G \text{ (m}^2 \text{ s}^{-1}\text{)}$		$D_M = D_G \varepsilon / \tau \text{ (m}^2 \text{ s}^{-1}\text{)}$		$\varepsilon / \tau$
$\Delta r \text{ (m)}$	$\Delta z \text{ (m)}$	$\Delta t \text{ (s)}$	HCHO	Water	HCHO	Water	$2.1 \times 10^{-1}$
$10^{-4}$	$10^{-4}$	$10^{-4}$	$1.67 \times 10^{-5}$	$2.4 \times 10^{-5}$	$3.5 \times 10^{-6}$	$5.03 \times 10^{-6}$	

**Fig. 4** Mass balance in an element of tube in gaseous phase (1A) and in contact with adsorptive phase (1B)



## Modeling approach

Mass transfer study is based on Fick's laws for the diffusion of formaldehyde and water vapor in the gas phase and through porous membrane (diffusion barrier). Due to the high permeability of the porous media ( $5.5 \times 10^{-12} \text{ m}^2$ ), these laws are suitable for this study case [29]. For formaldehyde, a concentration gradient in gas phase is considered from the sampling surface where the gas concentration is assumed to be zero due to sink effect of trapping media to air surrounding the diffusive sampler. For water vapor, adsorption equilibrium at the gas/solid interface is also taken into account. A control-volume method is implemented to develop the model.

### Gas phase and porous membrane mass transfer

For the development of the equation, it is considered an element (tube) located from these radial and axial coordinates  $r, z$  of radial thickness  $\Delta r$  and axial height  $\Delta z$ , as shown in Fig. 4, according to the geometry of the passive samplers (Fig. 3). The flow in these samplers is mainly radial, but it is essential to take account the axial diffusion because the heights of the monolith and the membrane (6 and 10 mm, respectively) are different. Moreover, the heterogeneous distribution of

formaldehyde concentration in the internal gas volume must be not neglected.

The main inlet parameters of the computer program are presented in Table 1.

Radial and axial diffusive flows ( $F_{ri}$ ,  $F_{ro}$ ,  $F_{ai}$ ,  $F_{ao}$ ) entering and leaving the element and are described hereafter:

$$F_{ri} = D_G \left( 2\pi \left( r + \frac{\Delta r}{2} \right) \Delta z \right) \left( \frac{dC}{dr} \right)_{r+\Delta r/2, z} \quad (1)$$

$$F_{ro} = D_G \left( 2\pi \left( r - \frac{\Delta r}{2} \right) \Delta z \right) \left( \frac{dC}{dr} \right)_{r-\Delta r/2, z} \quad (2)$$

$$F_{ai} = D_G (2\pi r \Delta r) \left( \frac{dC}{dz} \right)_{r, z-\Delta z/2} \quad (3)$$

$$F_{ao} = D_G (2\pi r \Delta r) \left( \frac{dC}{dz} \right)_{r, z+\Delta z/2} \quad (4)$$

Mass balance leads to the following equation:

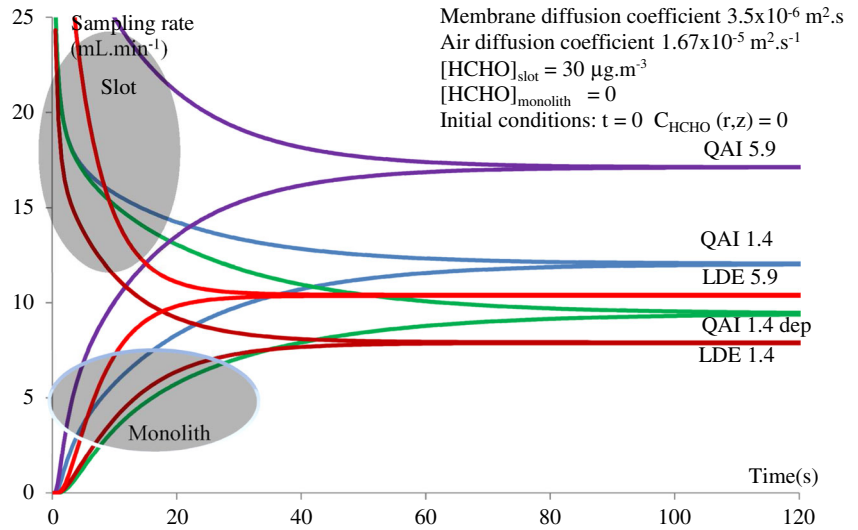
$$F_{ri} + F_{ai} - F_{ro} - F_{ao} = V_{r,z} \left( \frac{dC}{dt} \right)_{r,z}$$

$$\frac{D_G}{r} \frac{d}{dr} \left( r \frac{dC}{dr} \right)_{r,z} + D_G \left( \frac{d^2 C}{dz^2} \right)_{r,z} = \frac{dC}{dt} \quad (5)$$

**Table 3** Results on the sampled material flow ( $F_{\text{HCHO}}$ ), experimental sampling rate of formaldehyde ( $\text{SR}_{\text{exp}}$ ) for the different passive samplers and modeled sampling rate of formaldehyde ( $\text{SR}_{\text{mod}}$ ) under standard conditions: exposure time of 1 day  $[\text{HCHO}] = 30 \text{ ppb}$ ,  $\text{HR} = 50 \%$ , and  $T = 20 \text{ }^\circ\text{C}$

Passive sampler	$F_{\text{HCHO}}$ ( $\mu\text{g min}^{-1}$ ) Standard deviation	$\text{SR}_{\text{exp}}$ ( $\text{mL min}^{-1}$ ) Standard deviation	$\text{SR}_{\text{mod}}$ ( $\text{mL min}^{-1}$ )
QAI 1.4	$2.93 \times 10^{-4}$ $0.50 \times 10^{-4}$	11.76 1.83	12.03
QAI 5.9	$4.18 \times 10^{-4}$ $0.29 \times 10^{-4}$	17.44 1.97	17.10
LDE 1.4	$2.49 \times 10^{-4}$ $0.47 \times 10^{-4}$	8.84 0.94	7.90
LDE 5.9	$2.84 \times 10^{-4}$ $0.45 \times 10^{-4}$	10.03 0.17	10.37
QAI 1.4dep	$2.58 \times 10^{-4}$	9.14	9.42

**Fig. 5** Changes in formaldehyde sampling rates of studied passive samplers versus time until steady state



with  $C$  the gas concentration of the compound in the element,  $D_G$  the molecular diffusion coefficient of formaldehyde or water vapor in gas phase. For the mass diffusion through the porous membrane, the coefficient  $D_G$  was replaced by an effective diffusion coefficient  $D_M$ , adjusted from experimental kinetics.

Boundary conditions:

According to the drawing of passive samplers presented on Fig. 2, boundary conditions are as follows:

$$\text{Diffusive slot(membrane external surface)} \quad C = C_0 \quad (6)$$

For formaldehyde,  $C_0 = 30 \mu\text{g m}^{-3}$  (20 °C 1 atm)

For water vapor,  $C_0 = 13.82 \text{ g m}^{-3}$  (80 % RH, 20 °C and 1 atm)

### Monolith external surface

For formaldehyde,

$$C_{1,z} = 0 \quad (7)$$

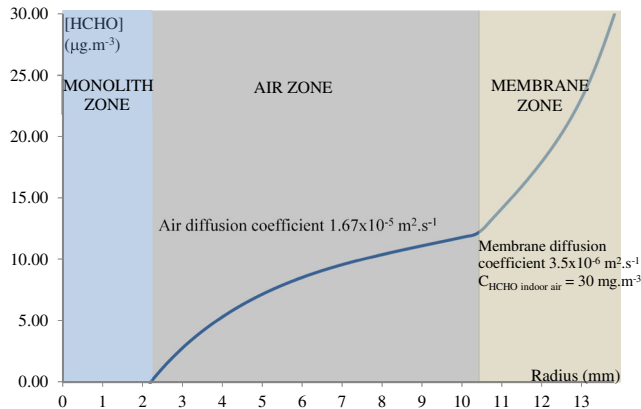


**Fig. 6** Radial distribution of formaldehyde concentration inside the QAI 1.4 passive sampler (axial location: center of diffusive slot)

For water vapor, the amount adsorbed  $q_z$  on the monolith in axial coordinate  $z$  is expressed as a function of the gas boundary layer concentration  $C_{1,z}$  by an adsorption equilibrium (Peleg isotherm) [30]:

$$q_z = \left( AC_{1,z}^C + BC_{1,z}^D \right) \frac{\Delta z}{h_{mon}} \quad (8)$$

where  $h_{mon}$  is the monolith height,  $A, B, C, D$  adjustment parameters of the isotherm data (Table 2). Sigmoid shape of the isotherm leads to application of Peleg model.

### Other boundary conditions:

$$\left( \frac{dC}{dr} \right)_z = 0 \quad \text{and} \quad \left( \frac{dC}{dz} \right)_r = 0 \quad (9)$$

Gas phase mass balance in an element in contact with the monolith considering the gas boundary concentration  $C_{1,z}$  located in  $r = r_{mon} + \Delta r/2$  with  $r_{mon}$  monolith radius (Fig. 4. 1B) is expressed as follows:

**Table 4** Results of the sensor response  $K$ ,  $K/m_{\text{HCHO}}$ , and  $K/\text{SR}$  in standard conditions

Passive sampler	$K$ (ppb <sup>-1</sup> min <sup>-1</sup> )	$K/m_{\text{HCHO}}$ (ppb <sup>-1</sup> min <sup>-1</sup> µg <sup>-1</sup> )	$K/\text{SR}$ (ppb <sup>-1</sup> mL <sup>-1</sup> )
QAI 1.4dep	$1.31 \times 10^{-6}$	$3.98 \times 10^{-7}$	$1.44 \times 10^{-7}$
LDE 1.4	$1.18 \times 10^{-6}$	$3.73 \times 10^{-7}$	$1.33 \times 10^{-7}$
LDE 5.9	$1.54 \times 10^{-6}$	$3.47 \times 10^{-7}$	$1.53 \times 10^{-7}$
Average		$3.73 \times 10^{-7}$	$1.43 \times 10^{-7}$
Standard deviation		$2.55 \times 10^{-8}$	$1.00 \times 10^{-8}$

$$F_{ri} + F_{ai} - \left( \frac{dq}{dt} \right)_{r_{mon,z}} - F_{ao} = V_{r,z} \left( \frac{dC_{1,z}}{dt} \right)_{r_{mon} + \Delta r/2,z}$$

$$D_{Gr} + \frac{\Delta r/2}{\Delta r \left( \frac{dC}{dr} \right)_{r_{mon} + \Delta r,z} + D_{Gr} \left( \frac{d^2 C_{1,z}}{dz^2} \right)_{r_{mon} + \Delta r/2,z} - \frac{1}{2\pi \Delta r \Delta z} \left( \frac{dq}{dt} \right)_{r_{mon,z}}} = r \left( \frac{dC_{1,z}}{dt} \right)_{r_{mon} + \Delta r/2,z} \quad (10)$$

$$\begin{aligned} \left( \frac{dq}{dt} \right)_{r_{mon,z}} &= \frac{dq_z}{dC_{1,z}} \frac{dC_{1,z}}{dt} \\ &= \frac{\Delta z}{h_{mon}} \left( ACC_{1,z}^{C-1} + BDC_{1,z}^{D-1} \right) \frac{dC_{1,z}}{dt} \end{aligned} \quad (11)$$

Initial conditions:

$t=0$ , for formaldehyde  $C_{r,z}=0$  and for water vapor  $C_{r,z}=8 \text{ g m}^{-3}$  (46 % RH, 20 °C and 1 atm).

Partial differential equations (Eqs. 5, 10) are transformed by substituting finite-difference approximations. The Alternating-Direction Implicit (ADI) scheme provides a mean for solving parabolic equations in two spatial dimensions using tridiagonal matrices [31]. The tridiagonal system is solved by LU decomposition in two steps. A personal computer program is implemented in Fortran 90 language to simulate the concentration distribution inside the gas sampler and the sampling rate as a function of time.

## Results and discussion

### Sampling rates of formaldehyde for the five passive samplers

Results on the sampled material flow and sampling rate of different passive samplers are summarized in Table 3. A good agreement is found for all studied cases between modeling and experimental results.

For the two types of sampler (QAI and LDE), the larger the width of the slot, more the mass transfer and the sampling rate of formaldehyde are increased (comparisons between QAI 1.4 and QAI 5.9, LDE 1.4 and LDE 5.9). The increase of mass transfer and sampling rate between the slots 1.4 and 5.9 is found higher for QAI sampler (+48 %) than for LDE sampler (+13 %). This difference could be due to an effect of internal volume and/or the distance between the diffusive slot and the membrane surface. To differentiate the influence of these two factors, the monolith position inside the sampler QAI 1.4 is modified with a translation of 1.2 cm on the vertical axis (QAI 1.4dep).

The sampling rate of QAI 1.4dep sampler is assessed to  $9.14 \text{ mL min}^{-1}$  corresponding to a reduction of about 29 %

compared to that of QAI 1.4 sampler ( $11.76 \text{ mL min}^{-1}$ ). Hence, the internal volume does not appear to be the main factor which can explain these sampling rate differences, but rather to be assigned to the membrane/monolith distance. This observation is in accordance with similar sampling rate values of LDE 1.4 and QAI 1.4dep samplers. As shown in Fig. 2, the two LDE samplers which have the highest membrane/monolith distance have also the lowest sampling rates. So the membrane/monolith distance is the main factor which explains the sampling rate of studied samplers. The modeling allows describing the sampling rate variation of studied passive samplers versus the time until steady state (Fig. 5). The time for establishment of steady state ranges from 30 to 110 s according to sampler (LDE 5.9 34 s, LDE 1.4 52 s, QAI 5.9 80 s, QAI 1.4 90 s and QAI 1.4dep 105 s). Consequently, the transient state corresponding to concentration variations should have a limited impact on the measurements with long-term sampling of several days. It is noted that the time for steady-state establishment is shorter when the sampler has both a small internal volume and a high sampling rate (case of LDE 5.9).

An additional test was carried out at 80 % RH in order to study the effect of humidity on the sampling rate of formaldehyde. For that, triplicate experiments were performed on the QAI 1.4 passive sampler under high humidity conditions. For

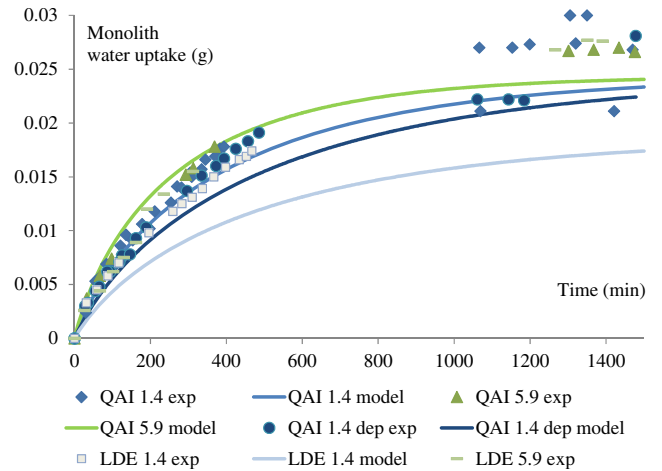


**Fig. 7** Adsorption kinetics of water vapor onto modified silica gel monolith ( $C_0 = 13.82 \text{ g m}^{-3}$ , 80 % RH, 20 °C, and 1 atm)

**Table 5** Results of the mass transfer of water ( $F_{H_2O}$ ) ( $t < 500$  min) and the water uptake on the monolith ( $m_{\text{monolith}}$ ) for 1 day with HR = 80 %,  $T^\circ = 20$  °C and  $[HCHO] = 0$  ppb

Passive sampler	$F_{H_2O}$ ( $\mu\text{g}/\text{min}$ )	$m_{\text{monolith}}$ (mg)
QAI 5.9	48.0	26.30
QAI 1.4	43.4	26.25
LDE 5.9	36.5	28.65
QAI 1.4dep	36.4	25.10
LDE 1.4	33.7	27.55

a relative humidity of 80 %, mass transfer of formaldehyde ( $F_{HCHO}$ ) is equal to  $2.75 \times 10^{-4} \pm 0.02 \times 10^{-4} \mu\text{g min}^{-1}$  and the sampling rate ( $SR_{\text{exp}}$ )  $12.60 \pm 0.25 \text{ mL min}^{-1}$ . In comparison with the experiments at 50 % RH ( $F_{HCHO} = 2.93 \times 10^{-4} \pm 0.50 \times 10^{-4} \mu\text{g min}^{-1}$  and  $SR_{\text{exp}} = 11.76 \pm 1.83 \text{ mL min}^{-1}$ ), the values are similar so humidity between 50 and 80 % RH has no effect on the sampling rate of formaldehyde. Low level of formaldehyde concentration ( $30 \mu\text{g m}^{-3}$ ) compared to high level of water ( $8.6 \text{ g m}^{-3}$  at 50 % RH and 20 °C) could explain the low effect of water vapor on formaldehyde sampling rate. This observation is only available for low formaldehyde concentration.

### Diffusion coefficient of formaldehyde through the membrane

The membrane is a diffusion barrier which allows controlling the sampling flow; its effect is taken into account considering the effective diffusion coefficient ( $D_M$ ). This coefficient is an adjustment parameter of model, deduced from previous experiments. Its value is equal to  $3.50 \times 10^{-6} \text{ m}^2 \text{ s}^{-1}$  as shown in Table 1. It can be expressed as a function of molecular diffusion ( $D_G$ ) and porosity/tortuosity ratio ( $\varepsilon/\tau$ ) by the expression  $D_M = D_G \varepsilon/\tau$  [32]. So the porosity/tortuosity ratio of the membrane can be estimated to  $2.1 \times 10^{-1}$ .

The modeled radial distribution of formaldehyde concentration inside the QAI 1.4 passive sampler in the center of diffusive slot is presented in Fig. 6. The observation of this

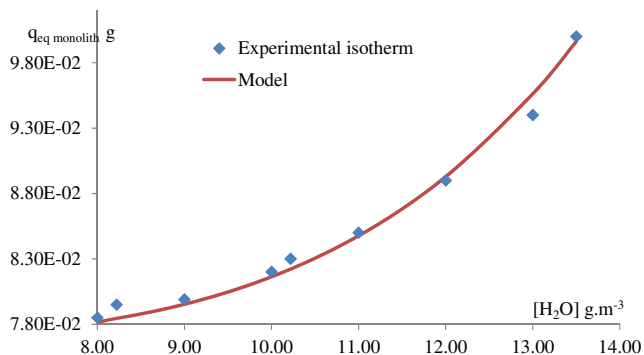


**Fig. 8** Adsorption isotherm of water vapor onto modified silica gel monolith

figure highlights a high concentration gradient at membrane boundaries, decreasing from 30 to  $12 \mu\text{g m}^{-3}$  (membrane thickness of 3.2 mm). However, sampling is not only governed by the mass transfer through the membrane because the internal boundary concentration is not close to 0. So the internal air diffusion has also an incidence on the global mass transfer. This conclusion is consistent with the different sampling rates of studied samplers due to their various membrane/monolith distances.

### Conversion factors between the sensor response and sampled formaldehyde mass/sampling rate

The absorbance change is proportional to the formed DDL amount, which is itself proportional to sampled formaldehyde amount. In the case of passive samplers using a sensor, the sampled formaldehyde mass cannot be directly assessed.

For this purpose, the sensor response noted  $K$  ( $\text{ppb}^{-1} \text{ min}^{-1}$ ) is defined as follows:

$$K = \frac{\Delta DO}{C \times t} \quad (14)$$

With  $\Delta DO$  the absorbance change measured before and after the sensor exposition,  $C$  formaldehyde concentration ( $\mu\text{g m}^{-3}$ ) and  $t$  the exposure time (min).

In the tests performed under standard conditions (reported in the section “Sampling rates of formaldehyde for the five passive samplers”), the absorbance changes ( $\Delta DO$ ) and the sensor responses ( $K$ ) may have been accurately assessed for only three of the five tested samplers (QAI 1.4dep, LDE 1.4, and LDE 5.9 passive samplers). From the results, relationships between the sensor response ( $K$ ), sampled mass formaldehyde ( $m_{HCHO}$ ) and sampling rate ( $SR$ ) were set up (Table 4).

The results of these tests lead to the assessment of conversion factors between  $K$  and  $m_{HCHO}$ :  $K/m_{HCHO} = 3.73 \times 10^{-7} \pm 0.26 \times 10^{-7} \text{ ppb}^{-1} \text{ min}^{-1} \mu\text{g}^{-1}$  and between  $K$  and  $SR$ :  $K/SR = 1.43 \times 10^{-7} \pm 0.10 \times 10^{-7} \text{ ppb}^{-1} \text{ mL}^{-1}$ . The conversion parameters ( $K/m_{HCHO}$  and  $K/SR$ ) are close for these three studied passive samplers.

### Water uptake trapped by monolith for the different passive samplers

In order to describe the mass transfer of water and the maximal water uptake of the monolith, each passive sampler is placed in a closed chamber where a follow up of the mass of the sensor is performed by weighing as described in the paragraph “Materials and methods” for two series. Results are summarized in Table 5 and Fig. 7.

The water uptake is quite similar for each passive sampler at equilibrium state. For all samplers, the sensor traps about 27 mg of water under high humidity conditions (80 % RH and

20 °C). Approximately 1000 min are needed to reach equilibrium. Differences in initial uptake rate ( $t < 500$  min) are observed between passive samplers. Comparing QAI and LDE for the same height of slot, the uptake rate of QAI is highest than that of LDE, confirming the incidence of membrane/monolith distance on mass transfer observed with formaldehyde. The results of the QAI 1.4 dep confirm this effect of the membrane/monolith distance. The model is quite in agreement with the experiments but it underestimates the water uptake kinetics of the LDE 1.4. The water adsorption isotherm of monolith, shown in Fig. 8, highlights the exponential shape of the curve at high humidity, characteristic of a capillary condensation inside the monolith.

## Conclusion

The aim of the present work is to evaluate diffusion parameters of five prototypes of passive samplers with different geometrical characteristics (slot width, internal volume, and membrane/monolith distance). The study of formaldehyde sampling rates showed that the main factors influencing the mass transfer are the slot width and the membrane/monolith distance. It was demonstrated that the effect of internal volume can be neglected compared with the membrane/monolith distance. Formaldehyde sampling rate was mainly governed by diffusion through the membrane but the diffusion in air volume inside the sampler has also an effect. This result is consistent with the incidence of membrane/monolith distance on formaldehyde sampling rate. An effective diffusion coefficient through the membrane ( $D_M$ ) was deduced from the model. Its value is equal to  $3.50 \times 10^{-6} \text{ m}^2 \text{ s}^{-1}$ . A porosity/tortuosity ratio ( $\epsilon/\tau$ ) of the membrane was evaluated to 0.21. Diffusive characteristics of the membrane will be specified in a future work; assessment of tortuosity will be mainly explored. Moreover, correspondences between the sensor response, sampled formaldehyde mass and sampling rate were assessed.

According to the good agreement between experimental and modeling results, the developed model is an efficient tool to optimize the design of new passive sampler, considering both formaldehyde sampling rate and water uptake trapped by monolith.

**Compliance with ethical standards** We wish to confirm that there are no known conflicts of interest associated with this publication and there has been no significant financial support for this work that could have influenced its outcome.

We confirm that the manuscript has been read and approved by all named authors and that there are no other persons who satisfied the criteria for authorship but are not listed. We further confirm that the order of authors listed in the manuscript has been approved by all of us.

We confirm that we have given due consideration to the protection of intellectual property associated with this work and that there are no impediments to publication, including the timing of publication, with

respect to intellectual property. In so doing we confirm that we have followed the regulations of our institutions concerning intellectual property.

We understand that the Corresponding Author is the sole contact for the Editorial process (including Editorial Manager and direct communications with the office). She is responsible for communicating with the other authors about progress, submissions of revisions and final approval of proofs. We confirm that we have provided a current, correct email address which is accessible by the Corresponding Author and which has been configured to accept email from valerie.desauziers@mines-ales.fr.

## References

1. Cartieaux E, Rzepka M, Cuny D. Indoor air quality in schools. *Arch Pediatr.* Jul. 2011;18(7):789–96.
2. Casset A, Marchand C, Le Calvé S, Mirabel P, De Blay F. Human exposure chamber for known formaldehyde levels: generation and validation. *Indoor Built Environ.* 2005;14(2):173–82.
3. Rancière F, Dassonville C, Roda C, Laurent AM, Le Moullec Y, Momas I. Contribution of ozone to airborne aldehyde formation in Paris homes. *Sci Total Environ.* 2011;409(20):4480–3.
4. Roda C, Guihenneuc-Jouyau C, Momas I. Environmental triggers of nocturnal dry cough in infancy: new insights about chronic domestic exposure to formaldehyde in the PARIS birth cohort. *Environ Res.* 2013;123:46–51.
5. Salthammer T, Mentese S. Comparison of analytical techniques for the determination of aldehydes in test chambers. *Chemosphere.* Dec. 2008;73(8):1351–6.
6. Schauer JJ, Kleeman MJ, Cass GR, Simoneit BRT. Measurement of emissions from air pollution sources. 4. C1–C27 organic compounds from cooking with seed oils. *Environ Sci Technol.* 2002;36(4):567–75.
7. Mitsubayashi K, Nishio G, Sawai M, Saito T, Kudo H, Saito H, et al. A bio-sniffer stick with FALDH (formaldehyde dehydrogenase) for convenient analysis of gaseous formaldehyde. *Sensors Actuators B Chem.* 2008;130(1):32–7.
8. Observatoire de la qualité de l'air intérieur (OQAI). Campagne nationale logements. Etat de la qualité de l'air dans les logements français. Rapport final. 2006.
9. Mariano S, Wang W, Brunelle G, Bigay Y, Tran-Thi T-H. Colorimetric detection of formaldehyde: a sensor for air quality measurements and a pollution-warning kit for homes. *Procedia Eng.* Jan. 2010;5:1184–7.
10. Kawamura K, Kerman K, Fujihara M, Nagatani N, Hashiba T, Tamiya E. Development of a novel hand-held formaldehyde gas sensor for the rapid detection of sick building syndrome. *Sensors Actuators B Chem.* Mar. 2005;105(2):495–501.
11. Lee C-Y, Chiang C-M, Wang Y-H, Ma R-H. A self-heating gas sensor with integrated NiO thin-film for formaldehyde detection. *Sensors Actuators B Chem.* Mar. 2007;122(2):503–10.
12. Xu J, Jia X, Lou X, Xi G, Han J, Gao Q. Selective detection of HCHO gas using mixed oxides of ZnO/ZnSnO<sub>3</sub>. *Sensors Actuators B Chem.* 2007;120(2):694–9.
13. Bunde RL, Jarvi EJ, Rosentreter JJ. A piezoelectric method for monitoring formaldehyde induced crosslink formation between poly-lysine and poly-deoxyguanosine. *Talanta.* 2000;51(1):159–71.
14. Feng L, Liu Y, Zhou X, Hu J. The fabrication and characterization of a formaldehyde odor sensor using molecularly imprinted polymers. *J Colloid Interface Sci.* 2005;284(2):378–82.
15. Demkiv O, Smutok O, Paryzhak S, Gayda G, Sultanov Y, Guschin D, et al. Reagentless amperometric formaldehyde-selective

- biosensors based on the recombinant yeast formaldehyde dehydrogenase. *Talanta*. 2008;76(4):837–46.
16. Martos PA, Pawliszyn J. Sampling and determination of formaldehyde using solid-phase microextraction with on fibre derivatization. *Anal Chem*. 1998;11(70):2311–20.
  17. Bourdin D, Desauziers V. Development of SPME on-fiber derivatization for the sampling of formaldehyde and other carbonyl compounds in indoor air. *Anal Bioanal Chem*. 2014;406(1):317–28.
  18. Zhang J, Zhang L, Fan Z. Development of the personal aldehydes and ketones sampler based upon DNSH derivatization on solid sorbent. *Environ Sci Technol*. 2000;732:2601–7.
  19. Descamps MN, Bordy T, Hue J, Mariano S, Nonglaton G, Schultz E, et al. Real-time detection of formaldehyde by a fluorescence-based sensor. *Procedia Eng*. Jan. 2010;5:1009–12.
  20. Maruo YY, Nakamura J, Uchiyama M, Higuchi M, Izumi K. Development of formaldehyde sensing element using porous glass impregnated with Schiff's reagent. *Sensors Actuators B Chem*. Feb. 2008;129(2):544–50.
  21. Descamps MN, Bordy T, Hue J, Mariano S, Nonglaton G, Schultz E, et al. Real-time detection of formaldehyde by a sensor. *Sensors Actuators B Chem*. Jul. 2012;170:104–8.
  22. Tran-Thi T-H, Dagnelie R, Crunaire S, Nicole L. Optical chemical sensors based on hybrid organic-inorganic sol-gel nanoreactors. *Chem Soc Rev*. Feb. 2011;40(2):621–39.
  23. Calvo-Muñoz ML, Truong TT, Tran-Thi TH. Chemical sensors of monocyclic aromatic hydrocarbons based on sol-gel materials: kinetics of trapping of the pollutants and sensitivity of the sensor. *J Mater Chem*. 2002;12:461–7.
  24. Chevallier E, Caron T, Belon C, Karpe P, Tran-Thi T.-H, Colomb S, Bigay Y. Development of a formaldehyde chemical sensor for indoor air quantification: Application in health and safety at work. *Conf Vent ParisFr* 2012.
  25. Nash T. The colorimetric estimation of formaldehyde by means of the Hantzsch reaction. *Biochem J*. Oct. 1953;55(3):416–21.
  26. Koziel JA, Noah J, Pawliszyn J. Field sampling and determination of formaldehyde in indoor air with solid-phase microextraction and on-fiber derivatization. *Sci Technol*. 2003;35:1481–6.
  27. Uchiyama S, Naito S, Matsumoto M, Inaba Y, Kunugita N. Improved measurement of ozone and carbonyls using a dual-bed sampling cartridge containing *trans*-1, 2-Bis (2-pyridyl) ethylene and 2, 4-dinitrophenylhydrazine-impregnated silica. *Anal Chem*. 2009;81(15):6552–7.
  28. Uchiyama S, Otsubo Y. Simultaneous determination of ozone and carbonyls using *trans*-1, 2-bis (4-pyridyl) ethylene as an ozone scrubber for cartridge. *Anal Chem*. 2008;80(9):3285–90.
  29. Webb SW, Pruess K. The use of Fick's law for modeling trace gas diffusion in porous media. *Transp Porous Media*. 2003;51(3):327–41.
  30. Peleg M. Assesment of a semi-empirical four parameter general model for sigmoid moisture sorption isotherms. *J Food Process Eng*. 1993;16(1):21–37.
  31. Chapra S, Canale R. *Numerical methods for engineers*. New-York: McGraw-Hil; 1988.
  32. Houst Y, Wittmann F. Influence of water content and porosity on the diffusivity of O<sub>2</sub> and CO<sub>2</sub> through hydrated cement paste. *Cem Concr Res*. 1994;24(6):1165–76.